HAL open science

A new method for the separation of waves. Application to the SHPB technique for an unlimited duration of measurement

Han Zhao, Gérard Gary

▶ To cite this version:

Han Zhao, Gérard Gary. A new method for the separation of waves. Application to the SHPB technique for an unlimited duration of measurement. Journal of the Mechanics and Physics of Solids, 1997, 45 (7), pp.1185-1202. 10.1016/S0022-5096(96)00117-2 . hal-00111583

HAL Id: hal-00111583

https://hal.science/hal-00111583v1

Submitted on 9 Nov 2022

HAL is a multi-disciplinary open access archive for the deposit and dissemination of scientific research documents, whether they are published or not. The documents may come from teaching and research institutions in France or abroad, or from public or private research centers.

L'archive ouverte pluridisciplinaire **HAL**, est destinée au dépôt et à la diffusion de documents scientifiques de niveau recherche, publiés ou non, émanant des établissements d'enseignement et de recherche français ou étrangers, des laboratoires publics ou privés.

Distributed under a Creative Commons Attribution - NonCommercial 4.0 International License

A NEW METHOD FOR THE SEPARATION OF WAVES. APPLICATION TO THE SHPB TECHNIQUE FOR AN UNLIMITED DURATION OF MEASUREMENT

HAN ZHAO and GÉRARD GARY

Laboratoire de Mécanique des Solides, Ecole Polytechnique. 91128 Palaiseau, France

The measuring duration of an SHPB (Split Hopkinson Pressure bar) set-up is limited by the length of the bars so that there is a limitation of maximum measurable strains in material testing applications. This paper presents a new two-gauge measurement method which takes account of the correction for wave dispersion effects, which cannot be ignored for long time measurements. Using bars of equal dimensions, it allows a quasi-unlimited measuring duration which can be up to 100 times longer than the classical one.

Analyses of the sensitivity of results to the imprecision of experimental data show that the method is robust and reliable. It is applied to the testing of soft materials like foam (metallic or polymeric) in the complete range of their response (nominal strains up to 80%) not only at high strain rates but also at medium strain rates ($5\,s^{-1} < \dot{\varepsilon} < 50\,s^{-1}$), with a measuring accuracy comparable with that of the SHPB. It is also successfully used to perform large displacement tests such as crushing of metallic tubes.

Keywords: A. dynamics, B. stress wave, B. viscoelastic material, C. Kolsky bar, C. impact testing.

1. INTRODUCTION

The SHPB (Split Hopkinson Pressure Bar) is a standard experimental technique nowadays for performing tests under dynamic loading. Its success is mainly due to the accuracy of its measurements. The technique finds its origin in the work of Hopkinson (1914) who used it to measure a pressure-pulse profile using a long thin bar and it has been well established since the critical study made by Davies (1948). The practical configuration with two long bars and a short specimen between them, widely used today, was introduced by Kolsky (1949). This technique, initially developed for compression tests, has been applied to tensile loading (Harding *et al.*, 1960) and to torsional loading (Duffy *et al.* 1971). To improve its precision, wave dispersion effects (Davies, 1948; Yew and Chen, 1978; Follansbee and Franz 1983; Gorham, 1983), three-dimensional effects (Davies and Hunter, 1963; Klepaczko, 1969; Dharan and Hauser 1970; Bertholf and Karnes, 1975; Malinowski and Klepaczko, 1986) and transient effects (Lindholm, 1964; Conn, 1965; Bell, 1966; Jahsman, 1971) in the specimen have been studied in the past dew decades.

The measuring technique using bars relies on the knowledge of the two elementary waves propagating in opposite directions. Once they are known, they can be time

shifted to the desired cross-section (bar specimen interfaces, for example) to calculate all the mechanical values, but the directly measurable quantities such as strains or velocities everywhere in a bar are the sum and the difference of the two elementary waves. The SHPB technique uses long bars and a short loading pulse so that a cross-section exists where the total incident pulse and the first part of reflected waves (of the same duration) can be recorded separately. A maximum observation duration then exists depending on the length of the bar and the measuring duration ΔT of a classical SHPB set-up is limited (Kolsky, 1963) to $\Delta T \leqslant L/C$, C being wave speed and L the length of the bar. Consequently, the total relative displacement Δl between the two bar–specimen interfaces is limited for a given loading speed V ($\Delta l \leqslant V\Delta T$). For material behaviour testing at a given average strain rate, the maximum measurable strain is limited ($\varepsilon_{max} \leqslant \dot{\varepsilon}\Delta T$). For instance, the measurable duration does not exceed 400 μs for an SHPB set-up made of 2-m long steel bars ($C \cong 5000$ m s^{-1}) and the measurable maximum strain is then limited to 20%, for a test performed at an average strain rate of about 500 s^{-1} (and only 1% for 25 s^{-1}).

The SHPB technique fails in two testing situations because the maximum strain attained is insufficient. One case is when the desired maximum strain (or total relative displacement) is very important. For example, in the study of the dynamic behaviour of polymeric or metallic foam, the desired maximum strain is often up to 80% to investigate the densification phenomenon of those materials. A large displacement during the test is also required for the study of the dynamic buckling of thin metallic tubes. In fact, specimens are effectively submitted to the desired strains (because of their low resistance) during the total time remaining after the observation window, but measurements are no longer possible after this time limit in a standard SHPB. Another case is when the desired strain rate is in the medium rate (5–50 s^{-1}). The technique cannot be applied because the maximum measurable strain becomes too small.

To increase the measuring duration of SHPB, some earlier workers have analysed the multiple reflections in bars. Campbell and Duby (1956) have reported a method on the basis of one-dimensional elastic wave theory. Lundberg and Henchoz (1977) have also proposed a simple explicit formula (within the one-dimensional wave propagation assumption) to separate the two elementary waves and to measure the particle velocity after the observation window, using two signals recorded at two different cross-sections in a bar. Recently, this method has found new application (Lundberg *et al.* 1990) in the prediction of wave propagation in a bar with a non-uniform impedance (due to a temperature gradient, for instance) and has been successfully used in high temperature SHPB testing (Bacon *et al.*, 1991, 1994; Lataillade *et al.*, 1994). However, as indicated by those authors (Campbell and Duby, 1956; Lundberg and Henchoz, 1977), such a method is valid only if the wave dispersion effect can be neglected. This situation is found when the bar is thin and the measuring duration is short (the duration in those works is about 1 ms for a bar of 10 mm diameter).

This paper presents a new measuring method on the basis of a similar analysis but without the above limitations. An iterative formula allowing for the calculation of the two virtually separate elementary waves for the total desired testing duration is presented in Section 2, using two signals recorded at two different cross-sections in each bar. It takes into account the wave dispersion effects which are very important

for accuracy in the case of a long time measurement. Some testing results on polymeric foam for a maximum strain up to 80% and on metallic tubes for a large crush are given in Section 3. The sensitivity of the present method to experimental perturbations is analysed in Section 4. It is found to be reliable in practical situations for a duration at least 100 times longer than the classical case. Tests on polymeric foam at medium strain rates (5–50 s^{-1}) are then possible and performed with a new testing set-up (here called the "slow bar" technique).

2. SEPARATION OF WAVES PROPAGATING IN OPPOSITE DIRECTIONS IN A HOPKINSON BAR

2.1. *Two-strain-gauge wave separation method*

The classical measuring technique using bars is based on the mechanics of elastic wave propagation in bars and on the superposition principle. (i) According to the elastic wave propagation theory, the stress, the strain and the particle velocity associated with a single wave are proportional to each other (with a sign depending on the propagating direction for the particle velocity). (ii) The knowledge of a single wave at a specific cross-section implies that it is known everywhere in the bar. (iii) Using the superposition principle in an elastic bar, the stress, the strain and the particle velocity at any cross-section can be considered as the algebraic sum of those values associated with the two elementary waves propagating in opposite directions at this cross-section.

Considering the two elementary waves in a bar, the wave propagating in the positive direction (arbitrarily defined) is named the "ascending" wave and the other one the "descending" wave (to avoid confusion with the classical SHPB, the terms "incident wave" and "reflected wave" are not used here). The strain $\varepsilon(t)$ at each section is the sum of the contribution of the elementary "ascending" wave $\varepsilon_{asc}(t)$ and that of the elementary "descending" wave $\varepsilon_{des}(t)$, and the velocity $v(t)$ is proportional to their difference:

$$\begin{aligned} \varepsilon(t) &= \varepsilon_{asc}(t) + \varepsilon_{des}(t), \\ v(t) &= C_0(\varepsilon_{asc}(t) - \varepsilon_{des}(t)), \end{aligned} \tag{1}$$

where C_0 is the wave speed.

At the section where the strain is measured, a prior knowledge of the contribution of one elementary wave will allow for the calculation of the other one.

Two strain gauges are cemented to distinct points A and B of the bar, as shown in Fig. 1. The strain histories at these two points, $\varepsilon_A(t)$ and $\varepsilon_B(t)$, are recorded. Since the bar is loaded at one end (by the projectile for the input bar and by the specimen for the output bar) while the other end remains at rest, the recorded signal at the first measuring cross-section A is due to a single elementary wave until the reflection at the other end comes back. The "ascending" wave at A, $\varepsilon_{ascA}(t)$ (because of the positive direction of the z-axis) is then equal to the measurement at point A, for the period $t < R_A$. It can be said for the same reason that the "descending" wave at point B,

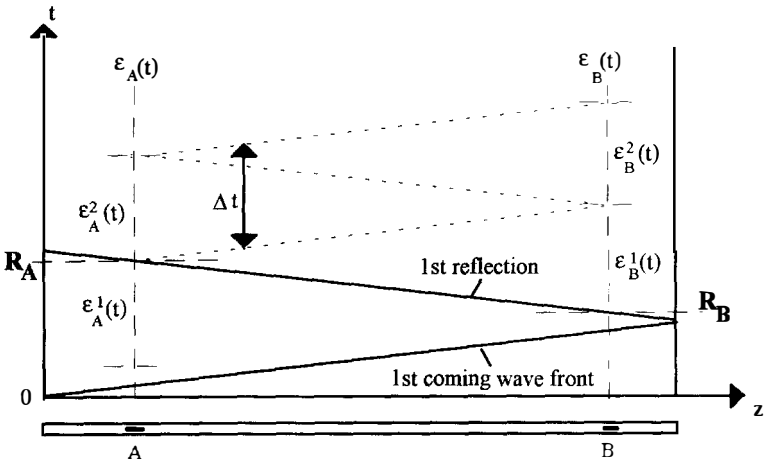

Fig. 1. Scheme for the separation of the waves.

$\varepsilon_{\mathrm{des}B}(t)$ is equal to zero for the period $t < R_B$ (Fig. 1):

$$\varepsilon_{\mathrm{asc}A}(t) = \varepsilon_A(t) \quad \text{if } t < R_A,$$
$$\varepsilon_{\mathrm{des}B}(t) = 0 \quad \text{if } t < R_B. \tag{2}$$

In order to exhibit "ascending" and "descending" waves from measurements at A and B which become afterwards mixtures of both elementary waves, an iterative process is built. Strain measurements $\varepsilon_A(t)$ and $\varepsilon_B(t)$ are divided into small pieces $\varepsilon_A^i(t)$ and $\varepsilon_B^i(t)$ of a constant time length Δt, as shown in Fig. 1. This interval Δt is twice the time needed by the waves to travel between the two gauges. In other words, $\varepsilon_A^1(t)$, $\varepsilon_A^2(t) \ldots \varepsilon_A^i(t)$ and $\varepsilon_B^1(t)$, $\varepsilon_B^2(t) \ldots \varepsilon_B^i(t)$ are obtained through the characteristic function of the intervals $[(i-1)\Delta t, i\Delta t]$ $(i = 1, 2, 3, \ldots)$:

$$\varepsilon_A^i(t) = \begin{cases} \varepsilon_A(t) & R_A + (i-2)\Delta t \leqslant t \leqslant R_A + (i-1)\Delta t \\ 0 & \text{otherwise} \end{cases},$$

$$\varepsilon_B^i(t) = \begin{cases} \varepsilon_B(t) & R_B + (i-1)\Delta t \leqslant t \leqslant R_B + i\Delta t \\ 0 & \text{otherwise} \end{cases}. \tag{3}$$

This operation can be applied to both virtual elementary "ascending" and "descending" waves at points A and B to obtain $\varepsilon_{\mathrm{asc}A}^i(t)$, $\varepsilon_{\mathrm{asc}B}^i(t)$, $\varepsilon_{\mathrm{des}A}^i(t)$ and $\varepsilon_{\mathrm{des}B}^i(t)$. According to (2), the "ascending" wave at A for $i = 1$ $(R_A - \Delta t \leqslant t \leqslant R_A)$, $\varepsilon_{\mathrm{asc}A}^1(t)$ is known. Knowing how the waves propagate, the "ascending" wave at point B can be found from the "ascending" wave at point A by applying the shifting function

$$\varepsilon_{\mathrm{asc}B}^1(t) = f_{\mathrm{shift}}(\varepsilon_{\mathrm{asc}A}^1(t)). \tag{4}$$

Using (1) at point B for $i = 1$ $(R_B \leqslant t \leqslant R_B + \Delta t)$, the corresponding part of the

"descending" wave at point B is

$$\varepsilon^{l}_{\mathrm{des}B}(t) = \varepsilon^{l}_{B}(t) - \varepsilon^{l}_{\mathrm{asc}B}(t). \tag{5}$$

The same process is performed to calculate the "ascending" wave at point A for the next interval from a knowledge of the "descending" wave given by (5). In this way, an iterative formula is constructed and both "ascending" and "descending" waves can be calculated for all the time intervals.

2.2. *Introduction of the wave dispersion correction in the iterative process*

Even for a classical SHPB set-up (where measured waves are at most shifted one length of the bar), the one-dimensional wave propagation theory has been shown not to be accurate enough (Davies, 1948; Follansbee and Franz 1983; Gorham, 1983; Gong *et al.*, 1990; Safford, 1992; Lifshitz and Leber, 1994). If the wave dispersion effects are not taken into account, the accuracy of the two-strain measurement method becomes rapidly insufficient with increase in the propagation distance, as indicated by Lundberg and Henchoz (1977) (see also an example in Section 2.3). Consequently, a more accurate propagation theory must be used, as it has already been introduced in the SHPB to improve the accuracy of the shifting process, taking account of so-called wave dispersion effects.

The analytical solution of the propagation of longitudinal waves in an infinite elastic bar obtained by Pochhammer (1876) and Chree (1889) has been used in different cases (Bancroft, 1941; Davies, 1948; Yew and Chen, 1978; Follansbee and Franz 1983; Gorham, 1983; Gong *et al.*, 1990; Lifshitz and Leber, 1994; Zhao and Gary, 1996). This solution has been extended to bars made of a linear viscoelastic material (Zhao and Gary, 1995). Such bars (made of nylon or PMMA) are needed to achieve an improved impedance ratio when soft material such as polymeric foam is studied. Even though Davies (1948) emphasized that the infinite bar theory is not exact, it has been verified in the usual SHPB set-up that it gives very good results.

It is therefore natural to use this wave propagation theory. Such an approach relies on the assumption that waves in the bar are harmonic so that all the associated mechanical variables can be described by their harmonic components. For instance, the strain $\underline{\underline{\varepsilon}}(z, t)$ can be expressed as follows:

$$\underline{\underline{\varepsilon}}(z, t) = \int_{-\infty}^{+\infty} \underline{\underline{\varepsilon}}^{*}(\omega) \mathrm{e}^{\mathrm{i}[\xi(\omega)z - \omega t]}\, \mathrm{d}\omega, \tag{6}$$

where the upper asterisk denotes frequency components of corresponding temporal functions.

The dispersion relation $\xi = \xi(\omega)$ between the wave number ξ and the frequency ω, describing the propagation of each frequency component, is defined through the so-called frequency equation derived from the solution for three-dimensional wave propagation in an infinite bar.

The signal $\varepsilon_A(t)$ or $\varepsilon_B(t)$ at section A or B is considered as the component ε_z of the

strain tensor $\underline{\underline{\varepsilon}}$ along the axis of the bar (z-axis). For any elementary wave, we have:

$$\varepsilon_A(t) = \varepsilon_z(z_A, t) = \int_{-\infty}^{+\infty} \varepsilon_z^*(\omega) e^{i[\xi(\omega) z_A - \omega t]} \, d\omega,$$

$$\varepsilon_B(t) = \varepsilon_z(z_B, t) = \int_{-\infty}^{+\infty} \varepsilon_z^*(\omega) e^{i[\xi(\omega) z_B - \omega t]} \, d\omega. \tag{7}$$

The wave shifting between A and B (separated by the distance $\Delta z = z_B - z_A$) consists in multiplying frequency components by a term depending on the dispersive relation

$$\varepsilon_B^*(\omega) = \varepsilon_A^*(\omega) e^{i\xi(\omega)\Delta z}. \tag{8}$$

Approach in the frequency domain. Since the wave shifting is defined in the frequency domain, it seems naturally easier to imagine a separating scheme in this domain. Indeed, the linearity of (1) shows that the frequency components of the strain can be expressed as the sum of the components of "ascending" and "descending" waves:

$$\varepsilon_A^*(\omega) = \varepsilon_{\mathrm{asc}A}^*(\omega) + \varepsilon_{\mathrm{des}A}^*(\omega),$$

$$\varepsilon_B^*(\omega) = \varepsilon_{\mathrm{asc}B}^*(\omega) + \varepsilon_{\mathrm{des}B}^*(\omega). \tag{9}$$

Using (8), we can substitute the "descending" wave at A by that at B and also the "ascending" wave at B by that at A so that (9) leads to:

$$\varepsilon_{\mathrm{asc}A}^*(\omega) = \frac{\varepsilon_B^*(\omega) - \varepsilon_A^*(\omega) e^{-i\xi(\omega)\Delta z}}{e^{i\xi(\omega)\Delta z} - e^{-i\xi(\omega)\Delta z}},$$

$$\varepsilon_{\mathrm{des}B}^*(\omega) = \frac{\varepsilon_A^*(\omega) - \varepsilon_B^*(\omega) e^{-i\xi(\omega)\Delta z}}{e^{i\xi(\omega)\Delta z} - e^{-i\xi(\omega)\Delta z}}. \tag{10}$$

However, it has been found difficult numerically to obtain sufficient accuracy with this method. On the one hand, a reliable evaluation of the high frequency components of the strain measurement, $\varepsilon_A^*(\omega)$ and $\varepsilon_B^*(\omega)$, needs a fast sampling rate whereas the evaluation of low frequency components needs a long observing duration. This leads to important data treatment. On the other hand, the denominator in (10) could become zero when an elastic bar is used [for $\xi(\omega)\Delta z = k\pi$, $\xi(\omega)$ being a real number]. It also nearly becomes zero for a viscoelastic bar. This problem is related to the inability of the set-up to "see" waves having a wavelength equal to the distance between two gauges. For all the frequencies near these singular points, it is difficult to obtain accurate results.

Approach in the time domain. For the time separating scheme presented in Section 2.1, the shifting function used in (4) is obtained with this wave propagation theory (8) and evaluated numerically using the Fast Fourier Transform (FFT):

$$f_{\mathrm{shift}}(\varepsilon_{\mathrm{asc,des}}^i(t)) = \mathrm{FFT}^{-1}[e^{i\xi(\omega)\Delta z}\mathrm{FFT}[\varepsilon_{\mathrm{asc,des}}^i(t)]]. \tag{11}$$

It is noted that the time separation scheme becomes theoretically inexact because of the incompatibility between the temporal cuts and the infinite stationary wave propagation theory. For example, the interval of duration Δt has been previously

defined as "twice the time needed by the waves for a travel between two gauges" but a common value with respect to the frequency components of Δt cannot be defined because the wave velocity now depends on the frequency. It is proved in Section 2.3 that such a separating scheme leads to a satisfactory result in our case.

Imprecision of calculations is unavoidable in the two methods and a major reason to prefer the time separation approach lies in the way results are affected. In the frequency separating scheme, errors are distributed everywhere in the time domain with an unknown local amplitude. The result, even at the time origin, could contain unknown and perhaps important errors. On the other hand, the temporal separating scheme produces cumulative errors so that the quality of the results only decreases with the distance virtually covered by the waves. The result within a certain distance is quite accurate (see Section 2.3), as can also be seen in Section 4.2, this point is very important in a real situation when perturbations of recorded signals are unavoidable.

2.3. *Validations*

Numerical simulations are used to show that the method itself and the associated numerical technique do not introduce significant errors and can be safely applied to real situations. Indeed, strain signals at A and B can be calculated from any given arbitrary ascending and descending elementary waves using the infinite bar propagation theory. With the present separation method, it is then possible to deduce ascending and descending waves from calculated signals (at A and B) and to compare them with initially given ones. The results of this approach do not show significant differences between initial and rebuilt signals (Zhao and Gary, 1994).

In order to test the overall efficiency of the method in a real situation, a bar with three strain gauges is used. Figure 2(a) shows the strain recordings at points A and B of a viscoelastic nylon bar. Using this new separation method, we can recover the strain history at any point of the bar. Figure 2(b) illustrates the comparison at C between the measured value and that recovered with the method (C was here chosen as the midpoint of the bar).

The nylon bar is only slightly viscous and the recorded signal is similar to what would be obtained with an elastic set-up. However, the one-dimensional elastic wave approximation (Lundberg and Henchoz, 1977) does not offer results of sufficient accuracy. Comparison between the recovered signal obtained within the one-dimensional elastic approximation and the measured signal is shown in Fig. 2(c). It proves that a more accurate description of the wave propagation is indeed necessary in this case.

3. APPLICATIONS TO SHPB TECHNIQUE TO IMPROVE MEASURING DURATION

3.1. *Behaviour of polymers and polymeric foam under dynamic loading*

Recently, a knowledge of the behaviour of low impedance materials (like foams) under crash situations has been needed in the automotive industry (Gary *et al.*, 1995) and has appeared as an important goal.

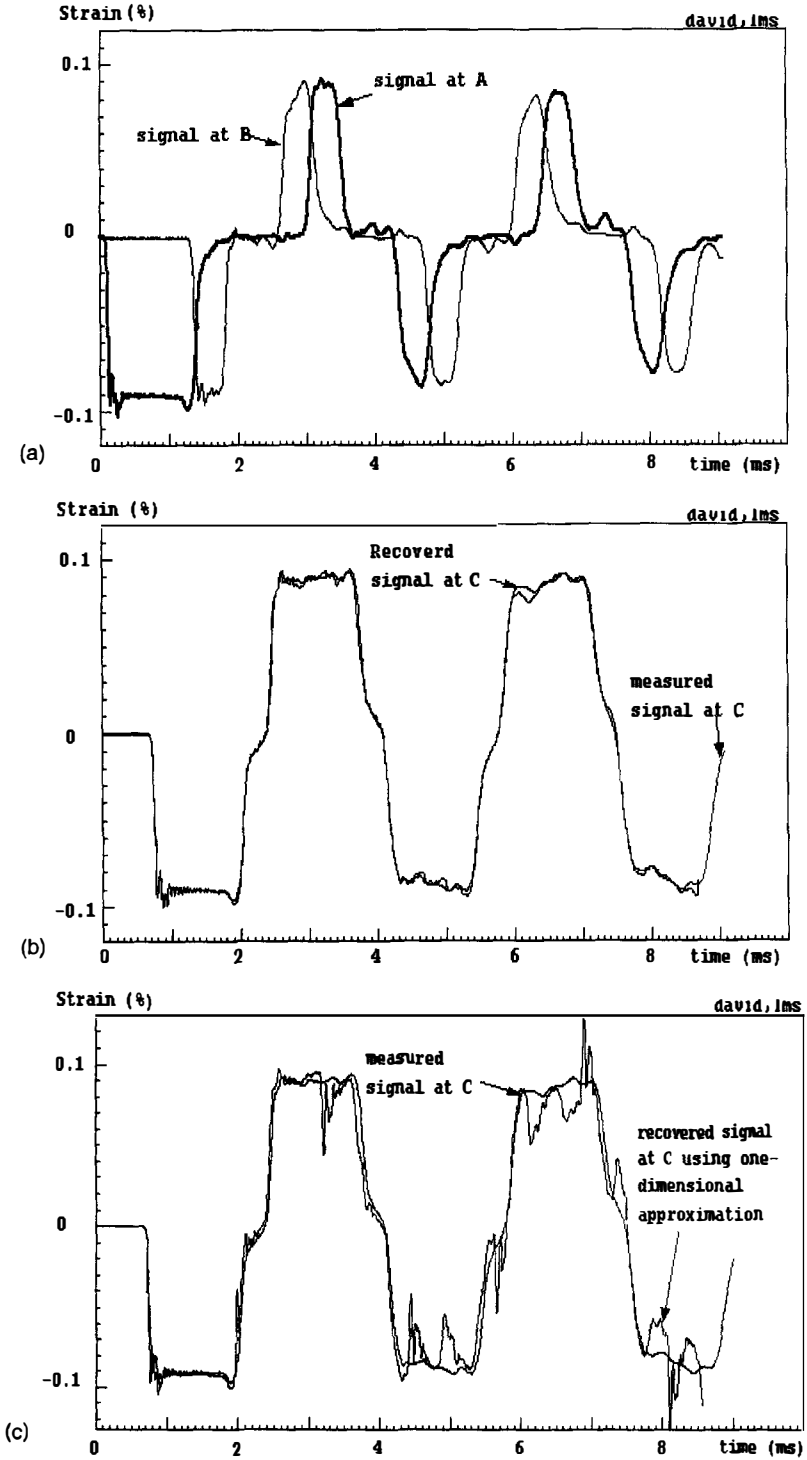

Fig. 2. (a) Direct measurements at points A and B. (b) Measurement at point C compared with reconstructed value. (c) Measurements at point C compared with theoretical values obtained using the one-dimensional approximation.

One particular feature of foam testing is the need for a large maximum strain (up to 80%) in order to study the densification part of the response, associated with a significant increase in the stress. In a conventional SHPB test at quite high strain rates of about 300 s^{-1}, it is not possible to measure such strains, even if they are easily reached after the measuring phase because of the very low resistance of foam. The difficulty associated with a limited measuring duration is solved with the wave separation method presented here.

A test on polymeric foam (a specimen of 40 mm length and 40 mm diameter) using a common nylon SHPB with two 3 m bars of diameter 40 mm is taken as an example. Two strain gauges (instead of one) are cemented onto the input and output bars. The four strain histories are recorded and shown in Fig. 3(a) (gauges 1 and 2 are on the input bar, gauges 3 and 4 on the output bar). One can recognize from the signal of gauge 2 that a common quasi-rectangular incident wave is launched by the projectile and that this pulse makes periodic round trips in the input bar.

The input and output velocities calculated from these signals are illustrated in Fig. 3(b). The measurable duration is about 12 ms, which is 10 times the initial SHPB measuring duration (about 1.2 ms) for this set-up. In terms of measurement duration, it is then as if two bars 30 m long had been used.

The deduced average stress–strain relation is shown in Fig. 3(c). The material behaviour is measured up to a strain three times larger than for a conventional SHPB. Since we have a periodic loading due to the round trip of the incident wave in the input bar, four loading–unloading cycles are observed. Unloading and reloading curves do not follow exactly the same path, which is in agreement with known material characteristics and gives confidence in the accuracy of the measurement. This ability to obtain dynamic loading–unloading cycles could be interesting for other viscoelastic materials or materials that accumulate damage. If the unloading has to be avoided, one just has to use a different and better adapted loading device, as indicated, for example, in Sections 3.2 and 4.

3.2. *Buckling of metallic tubes under dynamic loading*

Metallic thin tubes are widely used in the automotive industry, essentially as energy absorbers. Crush tests of tubes are usually made with a falling mass testing device. The deceleration of that mass is measured by an accelerometer. The associated force and displacement are then deduced, but the measuring precision is not always very good due to vibrations in the weight and its suspension system. Comparison between results for identical specimens tested by different devices of that type sometimes reveals differences of about 100% (Wierzbicki, 1995). More accurate results are obtained with a very long Hopkinson bar set-up (more than 100 m, Albertini *et al.*, 1993) but most laboratories do not have the space to do this.

It is thus of interest to use an SHPB system, known for its measuring precision, to test these kinds of structures. However, this application requires an SHPB bar with a large diameter to cover the tube section. In our laboratory, a large diameter (80 mm) SHPB system has been equipped to test geomechanical specimens such as rocks and concrete and is used for this application. In its classical version, this set-up with a 6 cm long input bar made of aluminium provides an observable applied displacement

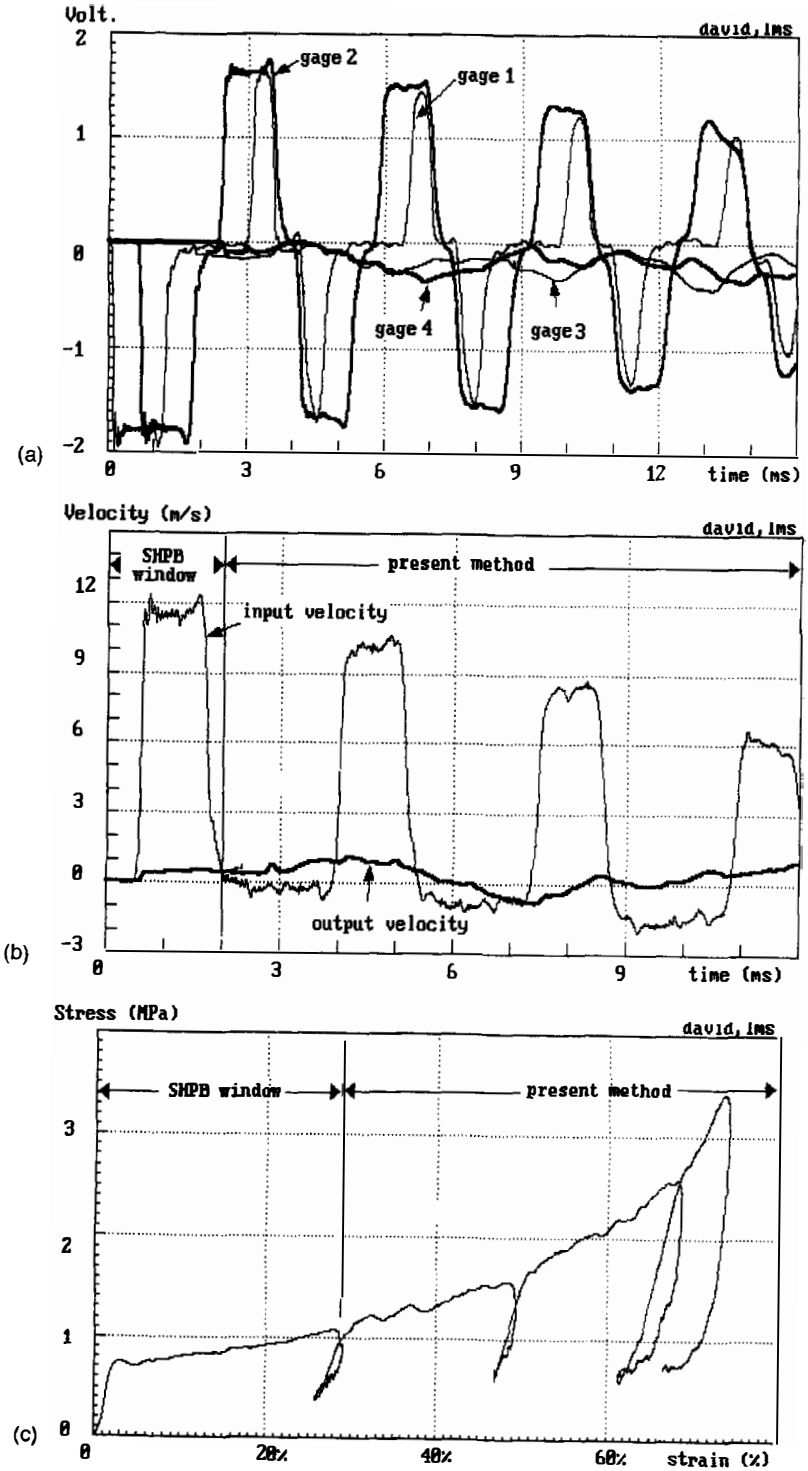

Fig. 3. (a) Recordings of four strain gauges cemented onto input and output bars. (b) Input and output velocities calculated from the four signals. (c) Average stress–strain relation for the foam.

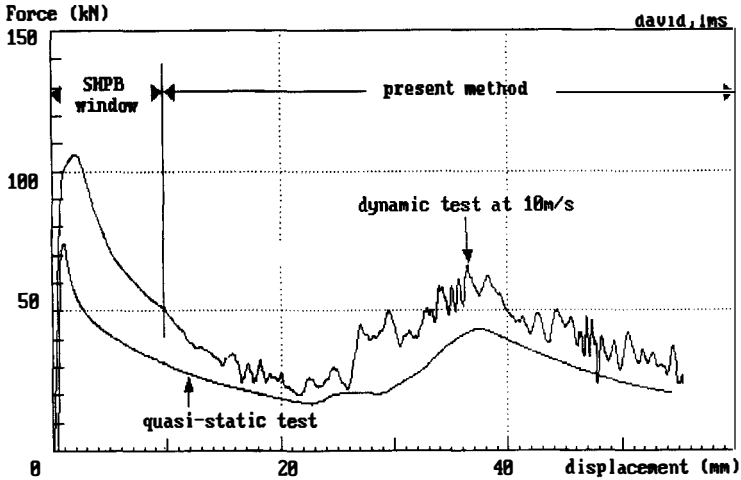

Fig. 4. Quasi-static and SHPB tests on an aluminium square thin tube.

of about 10 mm for an impact of 10 m s^{-1}. Using the new method presented in Section 2, tests of mini-structures can be performed with a large applied displacement.

Figure 4 shows test results on an aluminium 50 mm × 50 mm square tube (thickness 2 mm). A steel projectile of 3 m is used to produce a more important loading duration without unloading (the impacting side of the input bar remains loaded for a long time because the impedance of the projectile is greater than that of the input bar). The present method provides an observed crushing displacement of about 60 mm, six times greater than the displacement observed with the usual SHPB window.

Oscillations after the limit of the classical SHPB measurement are observed in the final force–displacement relation (the force–displacement relation shown in Fig. 4 is a raw result without any smoothing). Nevertheless, the precision in our case is much better than that obtained with a falling weight set-up.

However, the accuracy appears not to be as good as in the case of nylon bars. This could be due to the wave dispersion feature, more difficult to take into account here. Indeed, in a viscoelastic bar, the high frequency oscillations are progressively damped during propagation, whereas the wave dispersion effects in an elastic bar tend to increase the oscillations. Since the iterative recovering procedure is mainly based on the difference of two signals, the elimination of those increasing oscillations requires a more and more accurate shifting function with increase in shifting distance.

4. "SLOW BAR" TECHNIQUE

4.1. *Experimental arrangement of "slow bars"*

In studies related to passive security in the automotive or rail industry, strain rates involved in a crash situation are approximately situated between 5 s^{-1} and 1000 s^{-1}, and mostly in the low part of strain rates. It is important to have experimental data

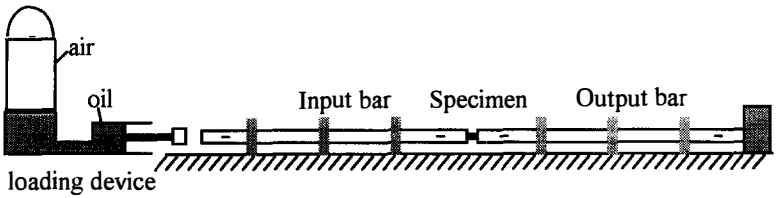

Fig. 5. "Slow bar" arrangement.

at medium strain rates (5–50 s^{-1}). For foam-like materials, tests in this range from 5 to 50 s^{-1} are generally performed with a fast hydraulic machine where a suitable measuring technique, often very expensive, is needed to obtain signals reflecting reality (Holzer, 1978).

The use of the SHPB measuring technique is thus proposed in this paper to perform tests at these medium strain rates. The method presented here theoretically has no limitation of duration. If a loading device can offer a sufficiently long push at a suitable quasi-constant velocity, tests at medium strain rates can be performed with satisfactory accuracy.

The difficulty of building such a loading device lies in the simultaneous requirement of sufficient impact energy and of a relative constant medium velocity. If a falling mass technique is used [see, for example, Baraya *et al.* (1965)], a huge mass is necessary to supply enough energy at a low velocity. If the technique of a cam driven by an engine (Loizou and Sims, 1953) or a hydraulic jack system is used, a huge installation is also needed to obtain a relatively constant velocity. The low cost system proposed here is an improved hydraulic oil jack (Fig. 5). It is composed of a hydraulic oil jack and a reservoir of compressed air to maintain the pressure in order to push at a relatively constant velocity.

Typical recordings of such a "slow bar" set-up are shown in Fig. 6(a). They concern a test without a specimen. The forces and the velocities at the bar–specimen interfaces calculated with the present method are shown in Fig. 6(b). The input values (force and velocity) are very close to the output ones, as it has to be for a test without a specimen.

A test with a "Slow bar" arrangement on the same polymeric foam as shown in Section 3.1 is illustrated in Fig. 7. Unloading is avoided due to the improved loading device.

4.2. *Sensitivity to measurement noise; some results on polymeric foam*

In the case of the test without a specimen shown in Fig. 6, we have observed that the calculated velocity is quite sensitive to differences between the amplifying coefficients of the two gauges on the same bar. As a quasi-static state in the two bars (equal forces without oscillations) is almost reached at the end of the test, it is possible to calibrate these coefficients so that the amplitudes of the four signals are equal at this moment. Such a possibility will not be realized in a real test and it is important to investigate the sensitivity of the results to those eventual imperfections.

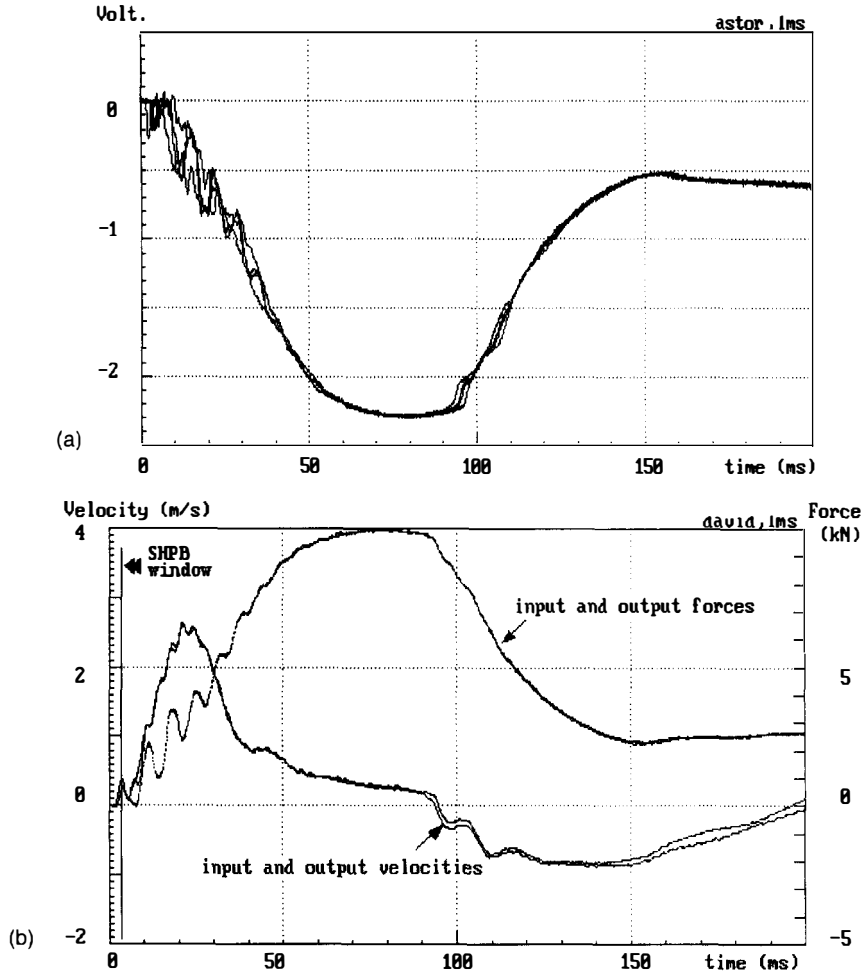

Fig. 6. (a) Recordings of four gauges of a "slow bar" set-up. (b) Input and output values calculated from four signals.

In order to evaluate this sensitivity, a random perturbation with an average non-null amplitude is added to one of the two recordings of each bar. In this way, a quantitative evaluation can be obtained. The average amplitudes of the perturbation that were studied were 0.5%, 1% and 3% of the current values of the signals. Such a choice is based on the consideration that an imprecision of 0.5% is hardly avoidable and an imprecision of 3% is commonly found. Figure 8(a) shows that the calculated force is not very sensitive to the perturbation. On the other hand, the calculated velocity is sensitive to it and a 0.5% perturbation introduces an important error. it must also be noted that the error on the calculated velocity is cumulative. During the first 40 ms, the velocity calculated from a signal with a 3% perturbation is still acceptable. The method using two strain gauges on each bar is then robust in the case

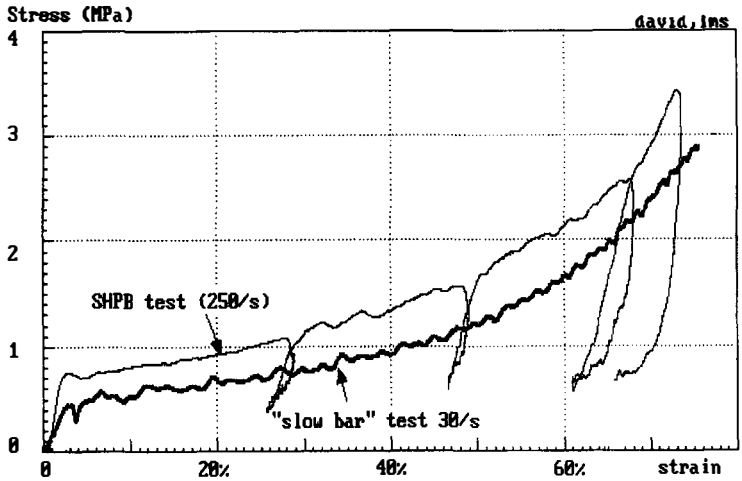

Fig. 7. Strain rate effects on foam at medium strain rates.

of the improved SHPB test presented in Section 3 where the duration is about 15 ms. it is also valid in the case of the "slow bar" test shown in Fig. 7 (about 30 ms).

In order to perform tests at even lower strain rates, another configuration of wave separation should be used. One can consider a natural configuration composed of a strain gauge and a velocity gauge. The separation scheme using a strain gauge and a velocity gauge is slightly different from that of two strain gauges but the theoretical basis is the same. It is expected that a direct measured velocity will prevent the calculated velocity from drifting. Using the recorded strain and a simulated velocity at the position of the other strain gauge, the force and velocity at the bar–specimen interfaces are again calculated, giving exactly the same result as when two strain gauges are used.

In order to study the sensitivity of a perturbation in this configuration, the same procedure as that used previously is applied. Figure 8(b) illustrates that a perturbation of an average amplitude of 3% on the velocity (or on the strain) does not introduce a significant error either on the force or on the velocity. It is noted that the two elementary waves could be directly known at the measuring point if the strain and the velocity could be measured exactly at the same cross-section. Such an approach is not investigated here because it has not been found easy to build such an arrangement practically.

A test on the same specimen as mentioned in Fig. 7 is performed at the same strain rate with the new arrangement of two strain gauges and two velocity gauges. Compared with results obtained with the four-strain-gauge arrangement, the local precision in such a configuration is not so good but the general result looks valid until the end of the test (Fig. 9). The observed oscillations are due to the insufficient accuracy of measured velocities, obtained by the numerical differentiation of the displacement signal given by an optical device.

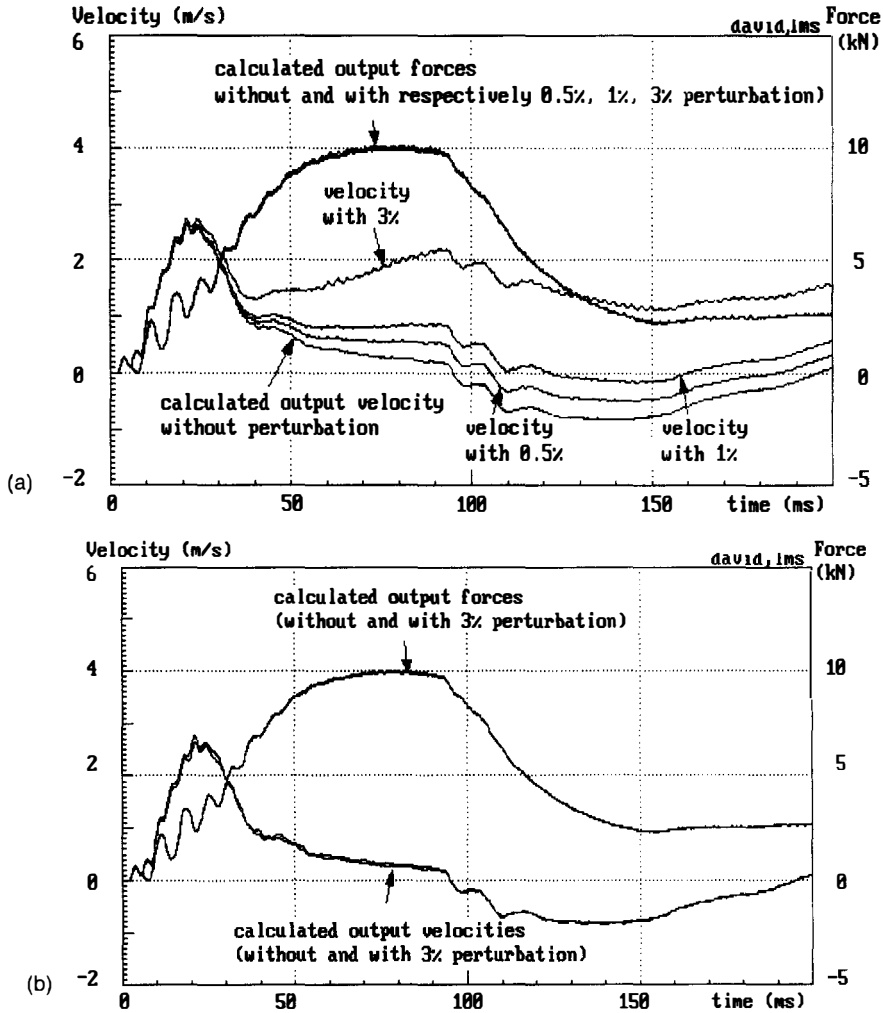

Fig. 8. (a) Two-strain measurement arrangement; sensitivity to experimental perturbations. (b) Strain and velocity measurement arrangement; sensitivity to experimental perturbations.

5. CONCLUSIONS

A new generalized two-gauge measurement method is presented in this paper in order to separate virtually the two elementary waves propagating in opposite directions in a bar. The proposed systematic iterative formula allows for the wave dispersion correction. It provides accurate results for a long observation time.

Using this method, the observing time duration of the measuring technique using bars, like SHPB set-ups, is almost unlimited. The application to common SHPB systems permits a significant increase (up to 100 times) in the measurement duration compared to a classical SHPB, so that it is possible to test mini-structures with significant displacements. For material testing applications, it is possible to measure

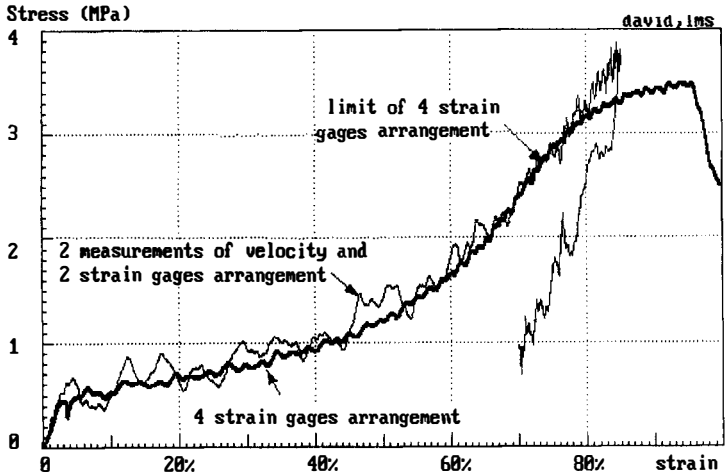

Fig. 9. Comparison between the two arrangements.

strains up to 80%, as required in testing polymeric or metallic foams. Using an appropriate loading device, a new possibility is also offered to perform tests at medium strain rates (5–50 s^{-1}). The most interesting perspective is found in this field. This technique allows precise measurements at medium strain rates, in a test range between the capabilities of a mechanical testing machine and classical Hopkinson bars.

REFERENCES

Albertini, C., del Grande, A., Delzano, A., Kiefer, R., Montagnini, M., Murarotto, M., Pizzinato, E. V., Rodis A. and Schnabel, A. W. (1993) New approach to crashworthiness studies of automotive and aerospace sheet metal structure by a large Hopkinson bar method. *Structure Dynamics* (*Eurodyn* 93), ed. T. Moan, P. G. Bergan, O. T. Gudmestad, C. M. Larsen, S. Nordal, S. Remseth, A. N. Nounadis, W. B. Krätzig and G. I. Schuëller pp. 539–545. AA Balkema, Rotterdam.

Bacon, C., Carlsson, J. and Lataillade, J. L. (1991) Evaluation of force and particle velocity at the heated end of rod subjected to impact loading. *J. Phys. IV* **C3,** 395–402.

Bacon, C., Färm, J. and Lataillade, J. L. (1994) Dynamic fracture toughness determined from load-point displacement. *Exper. Mech.* **34**(9), 217–223.

Bancroft, D. (1941) The velocity of longitudinal waves in cylindrical bars. *Phys. Rev.* **59,** 588–593.

Baraya, G. L., Johnson, W. and Slater, R. A. C. (1965) The dynamic compression of circular cylinders of super-pure aluminium at elevated temperatures. *Int. J. Mech. Sci.* **7,** 621–645.

Bell, J. F. (1966) An experimental diffraction grating study of quasi-static hypothesis of the SHPB experiments. *J. Mech. Phys. Solids* **14,** 309–327.

Bertholf, L. D. and Karnes, J. (1975) Two-dimensional analysis of the split Hopkinson pressure bar system. *J. Mech. Phys. Solids* **23,** 1–19.

Campbell, J. D. and Duby, J. (1956) The yield behaviour of mild steel in dynamic compression. *Proc. R. Soc. Lond.* **A236,** 24–40.

Chree, C. (1889) The equations of an isotropic elastic solid in polar and cylindrical co-ords, their solutions and applications. *Cambridge Phil. Soc. Trans.* **14,** 250–369.

Conn, A. F. (1965) On the use of thin wafers to study dynamic properties of metals. *J. Mech. Phys. Solids* **13,** 311–327.

Davies, E. D. H. and Hunter, S. C. (1963) The dynamic compression testing of solids by the method of the split Hopkinson pressure bar. *J. Mech. Phys. Solids* **11,** 155–179.

Davies, R. M. (1948) A critical study of Hopkinson pressure bar. *Phil. Trans R. Soc.* **A240,** 375–457.

Dharan, C. K. H. and Hauser, F. E. (1970) Determination of stress–strain characteristics at very high strain rates. *Exper. Mech.* **10,** 370–376.

Duffy, J., Campbell, J. D. and Hawley, R. H. (1971) On the use of a torsional split Hopkinson bar to study rate effects in 1100-0 aluminium. *J. Appl. Mech.* **38,** 83–91.

Follansbee, P. S. and Franz, C. (1983) Wave propagation in the split Hopkinson pressure bar. *J. Engng Mater. Technol.* **105,** 61–66.

Gary, G., Rota, L. and Zhao, H. (1995) Testing viscous soft materials at medium and high strain rates. *IUTAM Symposium on Constitutive Relation in High/Very High Strain Rates*, 16–19 October, NODA, Japan.

Gong, J. C., Malvern, L. E. and Jenkins, D. A. (1990) Dispersion investigation in the split Hopkinson pressure bar. *J. Engng Mater. Technol.* **112,** 309–314.

Gorham, D. A. (1983) A numerical method for the correction of dispersion in pressure bar signals. *J. Phys. E: Sci. Instrum.* **16,** 477–479.

Harding, J., Wood, E. D. and Campbell, J. D. (1960) Tensile testing of materials at impact rate of strain. *J. Mech. Engng Sci.* **2,** 88–96.

Holzer, A. J. (1978) A technique for obtaining compressive strength at high strain rates using short load cells. *Int. J. Mech. Sci.* **20,** 553–560.

Hopkinson, B. (1914) A method of measuring the pressure in the deformation of high explosives or by the impact of bullets. *Phil. Trans. R. Soc.* **A213,** 437–452.

Jahsman, W. E. (1971) Reexamination of the Kolsky Technique for measuring dynamic Material behavior. *J. Appl. Mech.* **38,** 77–82.

Klepaczko, J. R. (1969) Lateral inertia effects in the compression impact experiments. *Reports of Inst. Fund. Technical Research*, No. 17, Warsaw.

Kolsky, H. (1949) An investigation of the mechanical properties of materials at very high rates of loading. *Proc. Phys. Soc.* **B62,** 676–700.

Kolsky, H. (1963) *Stress Waves in Solids.* Clarendon Press, Oxford.

Lataillade, J. L., Bacon, C., Collombet, F. and Delaet, M. (1994) The benefit of Hopkinson bar of composite and ceramic materials. *Wave Propagation and Emerging Technologies*, ed. W. K. Kinra, R. J. Clifton and G. C. Johnson, ASME AMD-Vol. 188, pp. 85–93.

Lifshitz, J. M. and Leber, H. (1994) Data processing in the split Hopkinson pressure bar tests. *Int. J. Impact Engng* **15,** 723–733.

Lindholm, U. S. (1964) Some experiments with the split Hopkinson pressure bar. *J. Mech. Phys. Solids* **12,** 317–335.

Loizou, N. and Sims, R. B. (1953) The yield stress of pure lead in compression. *J. Mech. Phys. Solids* **1,** 234–243.

Lundberg, B. and Henchoz, A. (1977) Analysis of elastic waves from two-point strain measurement. *Exper. Mech.* **17,** 213–218.

Lundberg, B., Carlsson, J. and Sundin, K. G. (1990) Analysis of elastic waves in non-uniform rods from two-point strain measurement. *J. Sound Vib.* **137,** 483–493.

Malinowski, J. Z. and Klipaczko, J. R. (1986) Dynamic frictional effects as measured from the split Hopkinson bar. *Int. J. Mech. Sci.* **28,** 381–391.

Pochhammer, L. (1876) Uber die fortpflanzungsgeschwindigkeiten kleiner schwingungen in einem unbergrenzten isotropen kreizzylinder. *J. für die Reine und Angewande Mathematic* **81,** 324–336.

Safford, N. A. (1992) Materials testing up to $10^5\ s^{-1}$ using a miniaturised Hopkinson bar with dispersion corrections. *Proc. 2nd Int. Symp. on Intense Dynamic Loading and its Effects*, ed. Z. Guanren and H. Shihui, pp. 378–383. Sichuan University Press, China.

Wierzbicki, T. (1995) Material and Structural modelling in collision research *9th Dymat Technical Conference*, University of Technology, Munich (TUM). Germany.

Yew, E. H. and Chen, C. S. (1978) Experimental study of dispersive waves in beam and rod using FFT. *J. Appl. Mech.* **45,** 940–942.

Zhao, H. and Gary, G. (1994) Une nouvelle méthode de séparation des ondes pour l'analyse des essais dynamique. *C.R. Acad. Sci. Paris* **319,** série II, 987–992.

Zhao, H. and Gary, G. (1995) A three dimensional analytical solution of longitudinal wave propagation in an infinite linear viscoelastic cylindrical bar. Application to experimental techniques. *J. Mech. Phys. Solids.* **43**(8), 1335–1348.

Zhao, H. and Gary, G. (1996) On the use of SHPB techniques to determine the dynamic behavior of materials in the range of small strains. *Int. J. Solids & Struct.* **33**(23), 3363–3375.